Evaluation of fruit temperature on cherries by means of thermal point clouds

Evaluation of fruit temperature on cherries by means of thermal point clouds

Marco Bignardi
Dep. of Agromechatronics
Leibniz Institute for Agricultural Engineering and Bioeconomy,
Potsdam, Germany
https://orcid.org/0009-0002-2739-7004

Nikos Tsoulias
Dep. Of Agricultural Engineering Hochschule Geisenheim University
Geisenheim, Germany
https://orcid.org/0000-0002-6248-4333

Luigi Manfrini
Dep. Of Agricultural and Food Sciences (DISTAL)
University of Bologna
Bologna, Italy
https://orcid.org/0000-0003-4776-0608

Manuela Zude-Sasse
Dep. Of Agromechatronics
Leibniz Institute for Agricultural Engineering and Bioeconomy
Potsdam, Germany
https://orcid.org/0000-0002-8930-7855

***Abstract*— A LiDAR laser scanning and thermal imaging were employed to detect the temperature on sweet cherry surface ($T_{Estimated}$) by means of 3D point cloud. The LiDAR estimated temperature was temporally monitored in three varieties and compared with manually measured fruit temperature ($T_{Measured}$) and fruit fresh mass. The results showed correlation coefficients R^2 of 0.80 and 0.85 between estimated and measured temperatures of three different cultivars during the season. Related to fresh mass and the fruit quality data, T_{LiDAR} showed no correlation during the growing stages.**

Keywords— LiDAR, thermal camera, fruit temperature, precision orchard management

1. INTRODUCTION

Excessive sunlight and elevated temperature are the primary factors that can hinder the final yield and can induce stress on the outer skin of the fruits in orchards, including sweet cherries (*Prunus avium* L.). These environmental conditions impede the accumulation of anthocyanin, leading to reduced coloration on the fruit´s surface. These circumstances can also elevate respiration rates or hinder the overall process of photosynthesis, both of which impact the fruit´s growth during the cell division stage. Consequently, smaller-sized sweet cherries are produced. Temperatures between 35 °C to 40°C in post-fruit set, have been associated to impairments in keys physiological processes and up to 80 % yield loss [1, 2].

In this context, various two dimensional proximal and remote sensing techniques have been utilized [3, 4]. However, the implementation of proximal sensors has encountered certain challenges, particularly in terms of achieving consistent measurements across a large number of trees in commercial orchards. Moreover, expertise is required for sensor installation and maintenance, as well as the selection of suitable indices for detecting temperature in orchard environments [5, 6]. To overcome these limitations, remote sensing techniques offer a practical solution by enabling data collection from multiple trees within an orchard and employing automated data processing. The use of three-dimensional machine vision systems has gained attention in the field of horticulture, as they offer a solution to overcome the limitations of traditional two-dimensional imaging [7]. Whereas, non-invasive approaches of machine vision systems, which integrate thermal imaging and 3D point clouds by means of LiDAR laser scanner, have shown promising results in the field of horticulture [8, 9].

The main objective of this study was to accomplish three goals: asses the effectiveness of LiDAR with thermal data fusion approach in both (i) controlled laboratory settings and (ii) real-world field conditions and (iii) assess the temporal variations of LiDAR estimated fruit temperature with fruit properties.

2. MATERIAL AND METHOD

2.1 SITE DESCRIPTION AND PHENOLOGY

In 2022, an experiment was conducted in the sweet cherry orchard (Latitude: 52.466 °N, Longitude: 12.572 °E) at the Field Lab for Digital Agriculture of the Leibniz Institute for Agricultural Engineering and Bioeconomy (ATB) in Potsdam-Marquardt, Germany. The orchard has a North-South orientation (*Figure 1*). Three trees of three cultivars (n = 9) were selected based on the fruit skin colour: light red (*Prunus avium* cv: 'Napoleon'), dark red (*Prunus avium* cv: 'Adlerkirsche Von Bartschi'), and yellow (*Prunus avium* cv: 'Donissens Gelbe“'). The cultivars have been selected on their different skin color to assess possible variations in their temperature characteristics. The trees were trained as steep leader with

an average tree height of 3.2 m and 4 m distance between trees. Seasonal data have been collected at 55, 62 , 65, 73 and 83 days after full bloom (DAFB), respectively. Nine clusters of cherries were analyzed per each tree (n = 405) over the measuring dates. The clusters have been selected in three parts of the trees and on three heights from the ground to better characterize the distribution of the temperature in the canopy.

Figure 1: Satellite image of the cherry orchard, the studied trees are encased into the thick red polygon. Base image from ESRI World Map Background, Copyright © 1995 - 2023 ESRI

2.2 Sensing system

A rigid aluminium frame carrying the sensors was mounted on an inflexible linear tooth-belt conveyor system (Module 115/42, IEF Werner, Germany) of 0.8 m length, employing a servo positioning controller (LV-servoTEC S2, IEF Werner, Germany), to perform intrinsic and extrinsic calibration using an active pattern with clearly defined heat sources [7]. The linear conveyor moved at 20 mm s^{-1} (± 0.05 mm accuracy) forward speed. A mobile 2D LiDAR sensor with a wavelength of 905 nm (LMS-511, Sick AG, Waldkirch, Germany) coupled with a thermal camera (A655sc, FLIR Systems Inc., MA, USA) were used to acquire temperature annotated 3D point clouds (*Figure 2*) according to previous work [10].

The surface temperature of cherries was manually measured using an infrared thermometer (Microscanner D501, Exergen, Watertown, USA) in the three areas of each individual tree (n = 81). Whereas, a digitizer (Polhemus Fastrak, Inc., Colchester, VA, USA) was used to acquire the position of each cherry cluster. These measurements, referred to as ($T_{Measured}$), were then compared with the corresponding averaged temperature obtained by LiDAR ($T_{Estimated}$) at each individual tree area during the growth stages.

2.3 Fruit quality data

For fruit quality analysis, the sweet cherry clusters belonging in the middle height were collected from each tree on the five measuring dates (n = 135). The fresh mass (FM) [g] was measured by weighting each fruit sample. Moreover, chlorophyll, phenolic compounds, and specifically anthocyanin content was extracted per mg/100g of dry mass.

2.4 Data evaluation

Descriptive statistics were computed for all datasets, including minimum, maximum, mean, and standard deviation values. Both descriptive statistics and data visualization were done in Matlab by using Descriptive statistics (v.R2018b, Mathworks Inc., Natick, MA, USA).

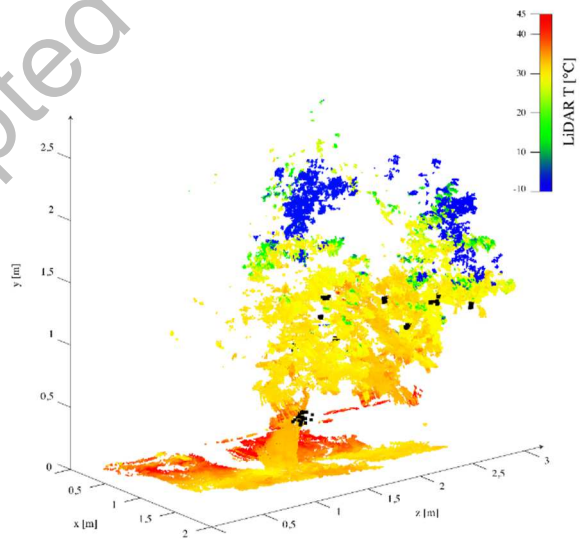

Figure 2: Representation of the 3D thermal point cloud and the position of the marked clusters with the digitizer (black dots) at DAFB73.

3. Results and discussion

3.1. Seasonal distribution of LiDAR temperature

The resulting thermal data sets of all cherries provided the fruit temperature estimated by means of LiDAR laser scanner ($T_{Estimated}$). The values ranged from 27 to 59 °C with a mean value of 41 °C, while the manually measured temperature on the skin surface ($T_{Measured}$) depicted a

range from 25 to 39 °C with a mean value of 32 °C considering all measuring days and all cherries (*Table 1*). A linear regression model described the relation between the latter two parameters, presenting an R^2 = 0.80, 0.80 and 0.85 with an 0.10, % 0.12 %, and 0.12 % RMSE, respectively for the Napoleon, Adlerkirsche von Bärtschi and Dönissens Gelbe (*Figure 3*). Despite the high bias, which can be corrected, the results are of practical interest, showing high correlation between measured and estimated fruit temperature. The correlation coefficients decreased when confronting the two datasets per date (Table 1). This could be due to the fluctuations of the air temperature that occur throughout the day. Furthermore, the RMSE values showed a slight increase during the days with higher detected temperatures, as well as the bias. This behavior could indicate that the sensing system could have a certain susceptibility to overestimation in hotter environment or the high global radiation may have caused a very rapid change of fruit temperature and a gap between LiDAR-based and manual measurements.

.

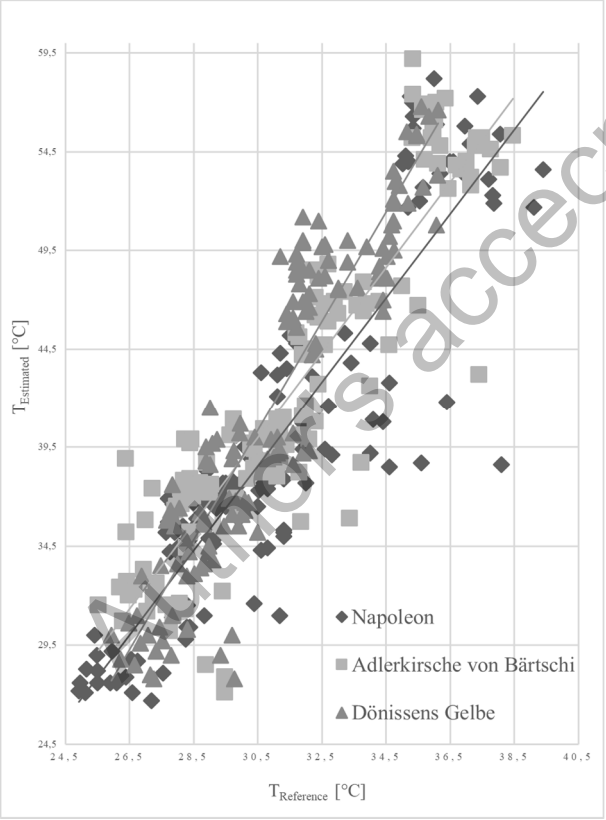

Figure 3: Scatter plots of the correlation between measured and estimated temperatures of the three different cultivars throughout the measured period.

Table 1: Descriptive statistics comparing manually ($T_{Measured}$) measured temperature and estimated fruit temperature ($T_{Estimated}$) based on LiDAR-derived temperature annotated point clouds (n = 9 per date and cultivar).

		DAFB 55	DAFB 62	DAFB 65	DAFB 73	DAFB 83
$T_{Estimated}$ [°C]	Min	27.8	34.4	43.2	26.7	34.3
	Max	40.1	51.2	59.2	41.5	46.9
	Mean	34.59	45.54	53.61	33.53	39.07
	RMSE (%)	0.07	0.13	0.18	0.06	0.09
	R^2	0.38	0.028	0.65	0.44	0.43
	Bias (%)	6.71	12.82	17.62	4.88	8.28

3.2 Fruit quality characteristics and LiDAR estimated temperature

Table 2: Descriptive statistics capturing, maximum (Max), minimum (Min), average (Mean) of fresh mass (FM), coefficient of determination (R^2) compared with LiDAR estimated temperature on fruit surface ($T_{Estimated}$).

	Date	Max	Min	Mean	R
Napoleon	$DAFB_{55}$	13.34	7.98	10.11	0.01
	$DAFB_{62}$	16.00	8.96	12.43	0.03
	$DAFB_{66}$	17.55	10.30	13.49	0.04
	$DAFB_{73}$	18.02	10.87	15.22	0.15
	$DAFB_{83}$	22.05	12.09	17.21	0.01
Adlerkirsche von Bärtschi	$DAFB_{55}$	13.34	7.72	11.88	0.07
	$DAFB_{62}$	20.11	9.39	15.57	0.62
	$DAFB_{66}$	23.75	10.57	16.97	0.25
	$DAFB_{73}$	25.19	13.69	19.74	0.01
	$DAFB_{83}$	29.05	13.29	20.68	0.04
Dönissens Gelbe	$DAFB_{55}$	10.40	7.02	8.36	0.04
	$DAFB_{62}$	17.42	10.28	13.17	0.03
	$DAFB_{66}$	18.28	10.53	13.95	0.20
	$DAFB_{73}$	22.80	12.40	17.58	0.64
	$DAFB_{83}$	25.44	12.24	17.28	0.31

The laboratory analysis showed that the fruit normally developed during the growing season (*Table 3*). Furthermore, the abovementioned quality data did not depict any correlation also with the measured temperatures.

No correlation was found between FM and $T_{Estimated}$ during the growing stages. During the lasts measuring dates, the yellow skin cultivar showed an increase in the correlation with the estimated temperature of 0.20, 0.64 and 0.31 and RMSE values of 0.19 %, 0.35 % and 0.22 %, respectively, during DAFB66, DAFB73 and DAFB83 (*Table 2*). Regarding the chlorophyll content as well as the phenolic compounds and the anthocyanins, also no correlation was found with the estimated temperatures.

Table 3: Descriptive statistics capturing, maximum (Max), minimum (Min), average (Mean) of Chlorophyll (Chl), Phenolic compounds (Pheo-a) and Antiochians (Cyanidin) content, coefficient of determination (R^2) compared with LiDAR estimated temperature on fruit surface (TEstimated).

	Quality parameter [mg/100g dry mass]	Max	Min	Mean	R
Napoleon	Chl	12.39	1.30	5.33	0.01
	Pheo-a	1.84	0.18	0.52	0.03
	Cyanidin	9.88	0	1.39	0.03
Adlerkirsche von Bärtschi	Chl	25.52	0.29	4.25	0.002
	Pheo-a	4.81	0.09	0.58	0.02
	Cyanidin	737.43	19.54	244.64	0.03
Dönissens Gelbe	Chl	17.46	0.61	6.39	0.12
	Pheo-a	2.99	0.19	0.85	0.22
	Cyanidin	0.0	0.0	0.0	0.0

4. CONCLUSION

The developed methodology enabled the alignment of thermal images with LiDAR-derived 3D point cloud in sweet cherries, achieving a low Root Mean Square Error (RMSE) of 0.10 RMSE/Pixel. This approach also yielded valuable insights into the fruit temperature derived from LiDAR ($T_{Estimated}$) on sweet cherry trees, which exhibited a strong correlation (R^2 = 0.85) with the manually measured fruit temperature ($T_{Reference}$) of the Napoleon cultivar. Notably, the T_{LiDAR} showed no correlation with FM, Chlorophyll, Phenolic compounds and Anthocyanins of the three varieties.

ACKNOWLEDGMENT

The project SHEET is part of the ERA-NET Cofund ICT-AGRI-FOOD, with funding provided by national sources [BLE] and co-funding by the European Union's Horizon 2020 research and innovation program, Grant Agreement number 862665.

4. REFERENCE

[1] Salvadores, Y., Bastías, R.M., 2023. Environmental factors and physiological responses of sweet cherry production under protective cover systems: A review. Chil. j. agric. res. 83, 484–498. https://doi.org/10.4067/S0718-58392023000400484

[2] Caprio, J.M., Quamme, H.A., 2006. Influence of weather on apricot, peach and sweet cherry production in the Okanagan Valley of British Columbia. Can. J. Plant Sci. 86, 259–267. https://doi.org/10.4141/P05-032

[3] M. Zude-Sasse, S. Fountas, T. Gemtos, and N. Abu-Khalaf, "Applications of precision agriculture in horticultural crops," *European Journal of Horticultural Science*, vol. 81, no. 2, pp. 78–90, Apr. 2016, doi: 10.17660/ejhs.2016/81.2.2.

[4] Tsoulias, N., Zhao, M., Paraforos, D.S., Argyropoulos, D. (2023). Hyper- and Multi-spectral Imaging Technologies. In: Zhang, Q. (eds) Encyclopedia of Smart Agriculture Technologies. Springer, Cham. https://doi.org/10.1007/978-3-030-89123-7_65-

[5] Gan, H., Lee, W. S., Alchanatis, V., & Abd-Elrahman, A. (2020). Active thermal imaging for immature citrus fruit detection. Biosystems Engineering, 198, 291-303. https://doi.org/10.1016/j.biosystemseng.2020.08.015

[6] Boini, Alexandra, Luigi Manfrini, Brunella Morandi, Luca Corelli Grappadelli, Stefano Predieri, Giulia Maria Daniele, and Gerardo López. "High levels of shading as a sustainable application for mitigating drought, in modern apple production." Agronomy 11, no. 3 (2021): 422. https://doi.org/10.3390/agronomy11030422

[7] Zude-Sasse, M., Akbari, E., Tsoulias, N., Psiroukis, V., Fountas, S., Ehsani, R. (2021). Sensing in Precision Horticulture. In: Kerry, R., Escolà, A. (eds) Sensing Approaches for Precision Agriculture. Progress in Precision Agriculture. Springer, Cham. https://doi.org/10.1007/978-3-030-78431-7_8

[8] Tsoulias, N., Jörissen, S., & Nüchter, A. (2022). An approach for monitoring temperature on fruit surface by means of thermal point cloud. MethodsX, 9, 101712.

[9] N. Tsoulias, A. Khosravi, W. Herppich, and M. Zude-Sasse, “Introduction of fruit water stress index by means of temperature annotated 3D point cloud” in press

[10] M. Zude-Sasse, L. Baranyai, and N. Tsoulias, “Spatio-temporal datasets of 3D thermal point clouds” in press.